

The Phase 1 Upgrade of the CMS Pixel Detector

Rong-Shyang Lu^{*†}

National Taiwan University

E-mail: Rong-Shyang.Lu@cern.ch

The LHC is running successfully, and it is expected that the instantaneous luminosity will surpass the design value of $10^{34}\text{cm}^{-2}\text{s}^{-1}$ before 2020. CMS has planned the so-called phase 1 upgrade between the two LHC long shutdowns to replace the current silicon pixel detector. The upgrade detector will be capable of fully exploiting the increased luminosity.

The upgrade detector will decrease the material budget significantly. The newly designed readout chip will improve the dead-time during high-rate and high-luminosity data taking. In this paper, we present the design of the upgrade detector along with the expected improvement and physics performance. The status of the project is also reported, including details of various detector components.

*The 21st International Workshop on Vertex Detectors - Vertex2012,
Sep. 16-21, 2012
Jeju, Korea*

^{*}Speaker.

[†]on behalf of CMS Collaboration

1. Introduction

The Compact Muon Solenoid (CMS) [1] experiment at the Large Hadron Collider (LHC) has provided excellent physics results since 2009. One of the key components of this success has been the good performance of the CMS tracking detectors, especially the pixel detector. Currently, the detector is running at high efficiency, with 96% of the channels functional, with a high hit efficiency of 99%, and good resolution [2]. The current pixel detector was designed to run at the LHC design luminosity of $10^{34}\text{cm}^{-2}\text{s}^{-1}$ for 2 years with expected fluences of up to $6 \times 10^{14}\text{cm}^{-2}$ 1 MeV neutron equivalent (N_{eq}) for the innermost layer before it is replaced. As LHC is running smoothly with a plan to exceed the design value before 2020, the current Readout Chip (ROC) will be facing excessive occupancy such that dead-time could exceed 50% if LHC runs at 50 nanosecond bunch spacing at an instantaneous luminosity of $2 \times 10^{34}\text{cm}^{-2}\text{s}^{-1}$. This immediately triggers the need for a new ROC and, therefore, a new pixel detector. At the same time, the performance of the detector will be improved by adding an extra layer and placing the innermost layer closer to the interaction point. Also in the new design, the overall material is decreased.

2. Design and Layout of the Upgrade Detector

The upgrade detector [3, 4] retains the same structure of barrel and endcap design, as shown in Fig. 1. The barrel detector contains four layers, one more layer than the current detector, at the radii of 30, 68, 109 and 160 mm. The barrel detector consists of 1216 pixel modules resulting in a total of 81 million pixel channels. The endcap detector contains three disks, one more disk than the current detector, on each side of the barrel detector. The three disks on each side allow for four-hits tracking up to ± 2.5 in pseudo-rapidity (η). The endcap detector consists of 672 pixel modules for a total of 44 million pixel channels. Each detector module on the outer ring of endcap is rotated by 20° in a turbine geometry. In order to obtain excellent resolution in both the azimuthal and radial directions throughout the endcap inner ring, the detector modules are arranged in an inverted cone array with the modules tilted by 12° with respect to the interaction point, combined with the 20° rotation.

The material budget of the upgrade detector is much reduced. The four-layer upgrade detector weighs 40% of the current three-layer detector, while the upgrade endcap detector weighs 80% of the current endcap detector. The service electronics, such as opto-electrical hybrids and power converters, are moved to a large z position, outside of the tracking volume of $|\eta| < 2.5$, thus reducing the radiation length to half of the current detector in the endcap region. The material budget in $|\eta| < 1.1$ is slightly reduced in radiation length, despite the fact that there is one more active layer.

3. Expected Performance

The expected physics performance of the proposed upgrade detector is studied for the LHC luminosity scenario of $2 \times 10^{34}\text{cm}^{-2}\text{s}^{-1}$. The gain in tracking performance can be seen when comparing to the current detector, as shown in Fig. 2, where a higher efficiency and a lower fake rate are observed. The efficiency is defined as the percentage of Monte-Carlo truth tracks that is

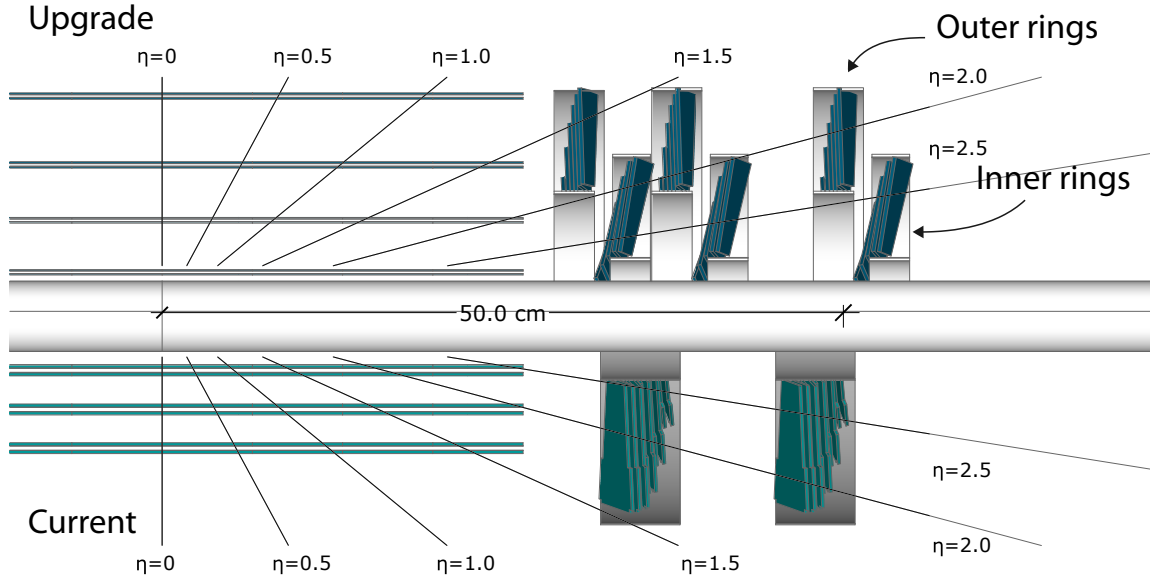


Figure 1: Layout of upgrade detector (top) and the current detector (bottom).

reconstructed where fake rate is the percentage of the reconstructed tracks that does not match to Monte-Carlo truth. The impact parameter (IP) resolution is also improved, as shown in Fig. 3 for the transvers impact parameter resolution as a function of track p_T for four different η region. The better tracking performance is due to a reduced data loss, reduced detector material and additional pixel layers, thus higher efficiency of track seeding, and a smaller radius on the innermost layer.

The performance of b-jet tagging is studied using the "Combined Secondary Vertex" algorithm [5], which is widely used in CMS. Various LHC luminosity scenarios were studied [4] and Fig. 4 shows the case of $2 \times 10^{34} \text{cm}^{-2} \text{s}^{-1}$ and 50ns bunch spacing, when the current pixel detector suffers a hit efficiency drop of $\sim 10\%$, depends on p_T and η , due to the data loss. Adding the effects of high pileup, the difference in b-tagging performance is further amplified. At a b-jet mistag rate of 1% for light quark jets, the b-jet tagging efficiency in the upgrade detector ($\sim 52\%$) is 31% higher than the current detector ($\sim 21\%$).

4. Status of the Project

The project aims to install and commissioning the detector in CMS during the extended technical stop of 2016/2017. A Technical Design Report [4] was released in Sep 2012. The production of modules and other components will start in 2014. The whole pixel detector will be assembled and be ready for installation in 2016. In the rest of this section, we describe the design, status and plan for various components of the detector.

4.1 Pixel Sensor

The pixel sensors use the same concept and design as the current CMS pixel sensor [6], as it has been proven to have good performance. The sensor is "n-on-n" with n^+ implants on a n

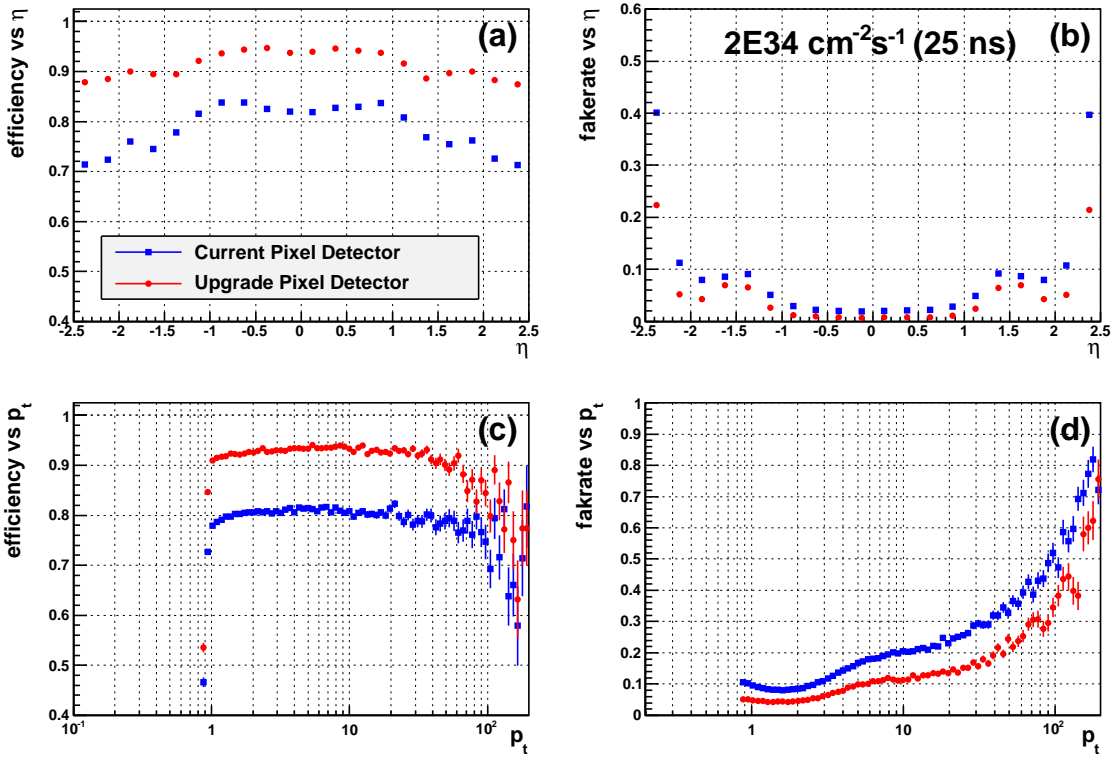


Figure 2: The tracking performance in $t\bar{t}$ MC sample of the upgrade detector (red) and current detector (blue) in the LHC operation scenario of an instantaneous luminosity of $2 \times 10^{34} \text{ cm}^{-2}\text{s}^{-1}$ and a bunch spacing of 25ns. The efficiency and fake rate are shown as functions of η or track p_T . The slight drop of efficiency in high Pt region comes from the dense jets of top quark decays. In this study, only pixel seeded tracks are reconstructed. The loss of efficiency is recovered by full tracking program.

bulk silicon. After irradiation induced space charge sign inversion, the highest electric field in the sensor is located close to the n^+ -electrodes used to collect the charge. This is an advantage that the not-fully-depleted operation is possible. The pixel dimensions are $100 \mu\text{m} \times 150 \mu\text{m}$ with a sensor thickness of $250 \mu\text{m}$. Current estimates [4] show that the sensor is capable of delivering enough signal for bias voltage of below 600V, even after receiving $1.5 \times 10^{15} \text{ N}_{\text{eq}}/\text{cm}^2$, corresponds to 250 fb^{-1} at a radius of 3 cm.

4.2 Readout Chip

There are several data-loss mechanisms in the current readout chip (ROC) architecture that need to be improved. The new ROC will be based on a 250nm CMOS process and have several new design features, listed below, that improve the performance :

- Readout protocol : The new ROC runs on internal 160MHz clock instead of 40MHz. A data serializer runs also on 160 MHz with a digital LVDS output driver. The digital readout removes the need for the complex decoding of a multilevel analog signal, which is the output format of the current ROC.

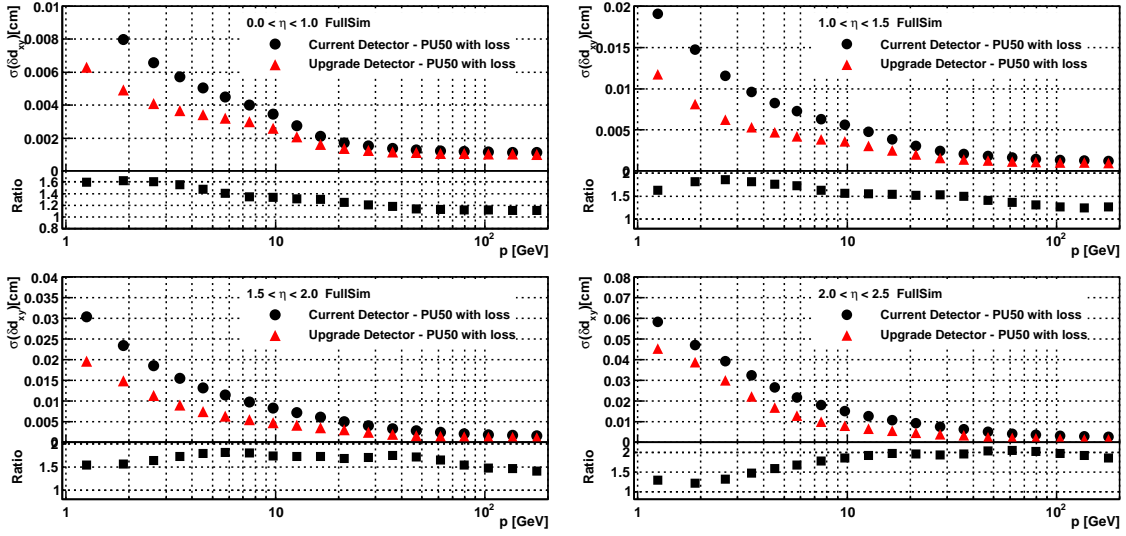


Figure 3: Transverse impact parameter resolution for muon tracks as a function of the track momentum for different η regions for the current pixel detector (black circles) and the Phase 1 upgrade detector (red triangles) for an average pileup of 50. The lower part of each plot shows the ratio of the current detector resolution to the upgrade resolution. (top-left) $0 < \eta < 1$; (top-right) $1 < \eta < 1.5$; (bottom-left) $1.5 < \eta < 2$; (bottom-right) $2 < \eta < 2.5$.

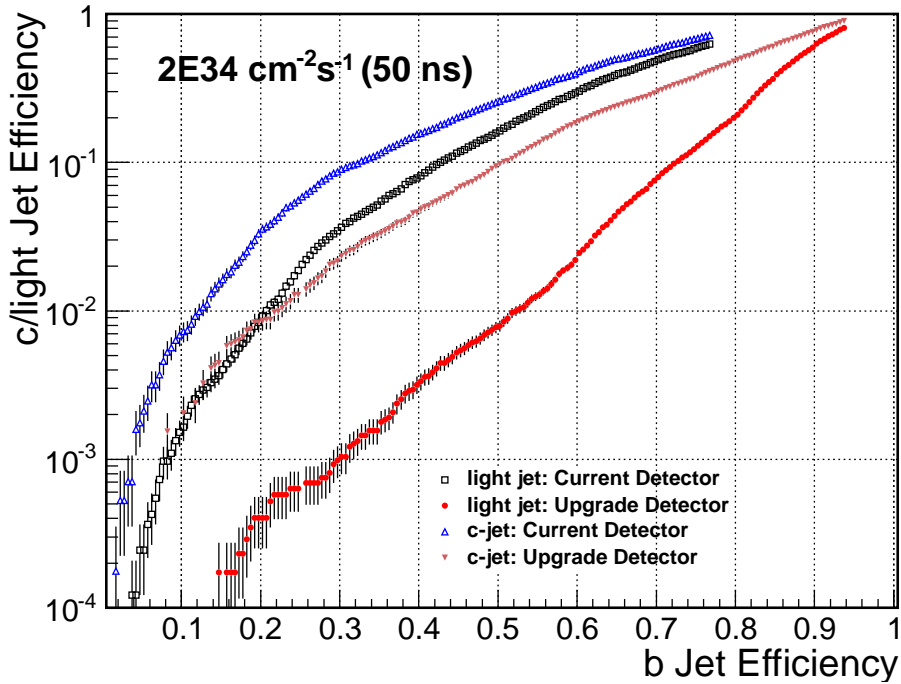


Figure 4: Performance of the Combined Secondary Vertex b -tagging algorithm for jets having $p_T > 30$ GeV in a $t\bar{t}$ sample with an average pileup of 100. The performance for the current detector is shown by the open points while the solid points are for the upgrade detector. The triangular points are for c -jets while the circle and square points are for light quark jets.

- **Reduced data loss** : The new ROC has an increased number of time stamp buffer cells (from 12 to 24) and data buffer cells (from 32 to 80) to reduce the probability of buffer overflow during data taking. An additional buffer stage on the ROC level has been introduced. Pixel hit data from the double columns start to be transferred to this new readout buffer immediately after the trigger signal is received. After being digitized, data wait there for the module readout to start. Simulation shows significant improvement on the data loss from either buffer overflow or column draining dead-time.
- **Enhanced analog performance** : Several improvements have been made to bring down the charge threshold, currently at 3500 electrons, of the ROC. This is higher than expected mainly from internal crosstalk. A new power distribution inside the ROC including an additional layout layer and thicker top layer have improved the crosstalk. Along with other minor improvements, this results in an absolute threshold well below 2000 electrons, as seen in the lab measurement.

4.3 Pixel Module

A pixel module contains 2×8 ROCs bump-bonded on a pixel sensors. The ROC peripheries with wire-bond pads extend 2 mm beyond the sensor along the two long sides of the module. A high density interconnect (HDI) is glued on top of the sensor with wire-bond pads to connect to the ROCs. The HDI provides signal and power distribution for the ROCs and carries the token bit manager chip (TBM). The TBM controls the readout of a collection of ROCs and distributes clock, trigger, reset signals and is the interface for directing the downloading of ROC operating constants. Two $250\mu\text{m}$ thick silicon nitride base-strips are glued to the back side of the ROCs and permit mounting of the modules on the mechanical structure. An illustration of the components of a pixel module is shown in Fig. 5.

4.4 Test-beam Experiment

Several test-beam experiments have been performed or are planned to study the ROC and pixel sensor performance in high-luminosity scenarios like that of the LHC environment. Several pixel sensors have been irradiated to $1.5 \times 10^{15} N_{\text{eq}}/\text{cm}^2$, corresponding to 250 fb^{-1} , and await testing in beams. There is also beam time assigned in 2012 and 2013 at CERN, DESY and FNAL to study the ROC performance under different particles types, energy, and fluence. Figure 6 shows an example of an eight-layer pixel telescope using eight single ROC module with digital ROCs in a proton beam line (H4) at CERN. An event display shows a track reconstructed using EUTelescope [7] software. Detailed analyses are being performed.

5. Summary

In preparation for the challenge of the high energy and luminosity era of LHC operation, CMS is upgrading the pixel detectors to fully exploit the luminosity. The upgrade detector will have one more layer of detectors, providing better tracking performance. The new ROC chip will cope with the important issue of data loss during the high luminosity and high pile-up scenario.

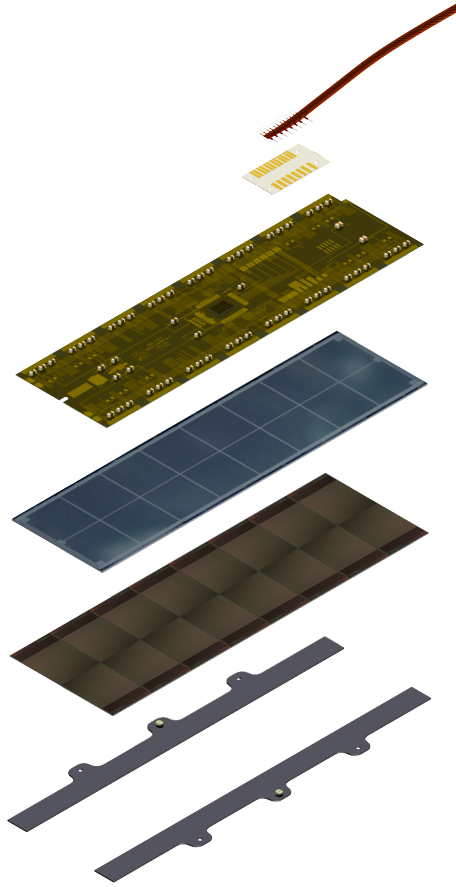


Figure 5: The composition of a pixel module for the upgrade detector. Components shown are, from top to bottom, the twisted pair cable and connector, the HDI, the pixel sensors, the ROCs and the base strips.

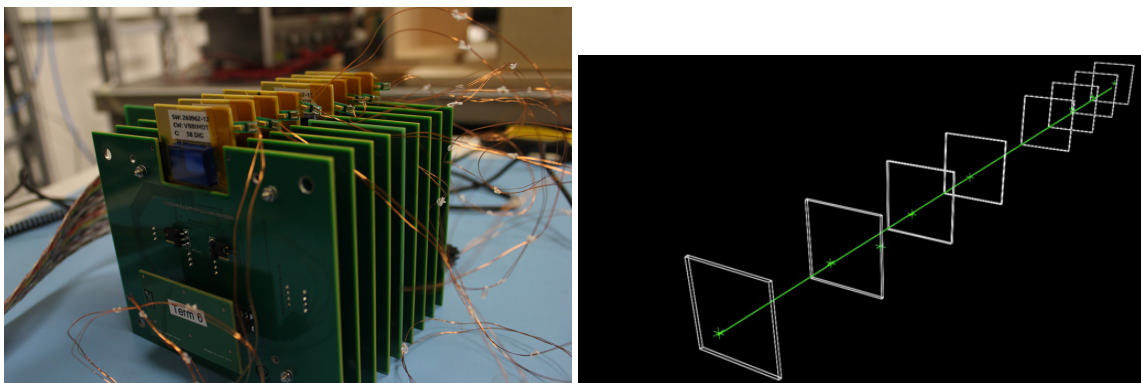


Figure 6: Left : Eight layer telescope with single-ROC modules mounted. Right : Event display showing a reconstructed track with energy deposited and measured on eight pixel sensors.

The upgrade project, at this moment, is joined by 12 funding agencies with 45 institutes around the world. Progress is seen on various R&D tasks to finalize the design of the detector. Module production is foreseen to start in 2014 and the target date for installation is the extended technical stop at the end of 2016.

References

- [1] CMS Collaboration, "The CMS experiment at the CERN LHC", JINST **3** (2008) S08004.
doi:10.1088/1748-0221/3/08/S08004
- [2] S. Zenz, "Operation and Performance of the CMS Silicon Strip Tracker", these proceedings.
- [3] "Technical Proposal for the Upgrade of the CMS detector through 2020", CERN-LHCC-2011-006 (2011).
- [4] "CMS Technical Design Report for the Pixel Detector Upgrade", CERN-LHCC-2012-016 (2012).
- [5] C. Weiser *et. al.*, "A Combined Secondary Vertex Based B-Tagging Algorithm in CMS", CMS Note CERN-CMS-NOTE-2006-014, CERN, (2010).
- [6] G. Bolla *et. al.*, "Sensor Development for the CMS pixel detector", Nucl. Inst. Meth. A 485(2002) 89-99.
- [7] I. Rubinskiy, "An EUDET/AIDA Pixel Beam Telescope for Detector Development", Physics Procedia 37 (2012) 923 - 931, <http://dx.doi.org/10.1016/j.phpro.2012.02.434>